



CHORUS

This is the accepted manuscript made available via CHORUS. The article has been published as:

Spin Torque Study of the Spin Hall Conductivity and Spin Diffusion Length in Platinum Thin Films with Varying Resistivity

Minh-Hai Nguyen, D. C. Ralph, and R. A. Buhrman

Phys. Rev. Lett. **116**, 126601 — Published 24 March 2016

DOI: [10.1103/PhysRevLett.116.126601](https://doi.org/10.1103/PhysRevLett.116.126601)

**Spin torque study of the spin Hall conductivity and spin diffusion length
in platinum thin films with varying resistivity**

Minh-Hai Nguyen¹, D. C. Ralph^{1,2}, R. A. Buhrman^{1*}

¹Cornell University, Ithaca, New York 14853, USA

²Kavli Institute at Cornell, Ithaca, New York 14853, USA

ABSTRACT

We report measurements of the spin torque efficiencies in perpendicularly-magnetized Pt/Co bilayers where the Pt resistivity ρ_{Pt} is strongly dependent on thickness t_{Pt} . The damping-like spin Hall torque efficiency per unit current density ξ_{DL}^j varies significantly with t_{Pt} , exhibiting a peak value $\xi_{\text{DL}}^j = 0.12$ at $t_{\text{Pt}} = 2.8 - 3.9$ nm. In contrast, $\xi_{\text{DL}}^j / \rho_{\text{Pt}}$ increases monotonically with t_{Pt} and saturates for $t_{\text{Pt}} > 5$ nm, consistent with an intrinsic spin Hall effect mechanism, in which ξ_{DL}^j is enhanced by an increase in ρ_{Pt} . Assuming the Elliott-Yafet spin scattering mechanism dominates we estimate that the spin diffusion length $\lambda_s = (0.77 \pm 0.08) \times 10^{-15} \text{ } \Omega\text{m}^2 / \rho_{\text{Pt}}$.

* rab8@cornell.edu

The spin Hall effect (SHE) [1–3], in which a transverse spin current density j_{SHE} is induced by a longitudinal charge current density j_e and whose strength is characterized by the spin Hall ratio $\theta_{\text{SH}} \equiv (2e/\hbar)j_{\text{SHE}}/j_e$, has recently drawn much attention because of its promise for spintronics applications [4–13]. Mechanisms which might give rise to the SHE [14,15] include the intrinsic SHE [1,16], side-jump scattering [17] and skew scattering [18]. Two common methods to quantify the strength of the SHE are to employ ferromagnet/normal metal (FM/NM) bilayers and either (1) detect the spin transfer torque that the SHE-induced spin current from the NM layer exerts on the magnetization of the adjacent FM layer [19,20], or (2) use spin pumping to inject a spin current from the FM to the NM and detect the electric current in the NM layer that is induced by the inverse SHE (ISHE) [21–23]. In the former case due to spin backflow (SBF) at the FM/NM interface [24,25] and/or enhanced spin scattering at the interface (spin memory loss or SML) [26], only a portion $j_s^{\text{NM|FM}}$ of the SHE-induced spin current j_{SHE} is absorbed in the FM layer, and that reduces the damping-like (DL) spin Hall (SH) torque efficiency per unit current density

$$\xi_{\text{DL}}^j \equiv (2e/\hbar)j_s^{\text{NM|FM}}/j_e = T_{\text{int}}\theta_{\text{SH}} \quad (1)$$

to be less than θ_{SH} , where $T_{\text{int}} = j_s^{\text{NM|FM}}/j_{\text{SHE}}$ (<1) is the interfacial spin transparency. SBF and/or SML can similarly reduce the strength of spin-pumping/ISHE signals.

Large values of ξ_{DL}^j have been reported for Pt [19,27–31], beta-Ta [19] and beta-W [4]. Special attention has been paid to Pt because its relatively low resistivity compared to the other SH materials would be beneficial for reducing Ohmic losses in applications. Values of ξ_{DL}^j for Pt have been reported spanning the range 0.06 - 0.12 [19,27–29], depending on the FM/Pt

interface [31], and are usually accompanied by a relatively small field-like (FL) torque efficiency whose magnitude and sign vary with the interface, FM magnetic anisotropy and temperature [29,32–36]. From an analysis of SBF based on a spin diffusion model [24,25], these ξ_{DL}^j results indicate that the underlying internal value of θ_{SH} for Pt is ~ 0.2 or even larger [28,29,31]. However, the determination of θ_{SH} from ξ_{DL}^j using the spin diffusion model requires an accurate value of the spin diffusion length λ_s , and in the case of Pt that value has long been controversial. Measurements by different techniques, at low and room temperatures, have reported a wide range, 1 - 11 nm, for λ_s in Pt [21–23,37–48]. Those measurements will be reviewed along with our analysis later in this Letter.

Here we report that ξ_{DL}^j has a strong, unexpected dependence on Pt thin film thickness t_{Pt} in perpendicularly-magnetized Pt/Co bilayers, as measured by the harmonic response (HR) technique [20,29]. In particular we report that ξ_{DL}^j exhibits a peak at $t_{\text{Pt}} = 2.8 - 3.9$ nm and gradually decreases at larger Pt thickness. This behavior is counter to the common expectation, reported in prior experiments with different layer structures [38,40,45], that ξ_{DL}^j should simply increase and saturate at a maximum value as t_{Pt} exceeds the spin diffusion length λ_s in Pt. Our interpretation of our result is that the spin Hall ratio is linearly dependent on the Pt resistivity ρ_{Pt} , which in turn varies approximately inversely with t_{Pt} in our samples in the thin Pt limit, $t_{\text{Pt}} \leq 4$ nm, due to strong diffusive scattering at the Pt interface(s). We observe that the spin-torque efficiency *per unit applied electric field*

$$\xi_{\text{DL}}^E \equiv (2e / \hbar) j_s^{\text{NM|FM}} / E = T_{\text{int}} \sigma_{\text{SH}} = \xi_{\text{DL}}^j / \rho_{\text{Pt}} \quad (2)$$

(E is the electric field in the Pt film) increases monotonically with t_{Pt} and saturates at $t_{\text{Pt}} \approx 5$ nm. This is consistent with a spin Hall conductivity $\sigma_{\text{SH}} \equiv (2e/\hbar)j_{\text{SHE}}/E$ that is independent of ρ_{Pt} , which indicates that the intrinsic SHE (and/or side-jump scattering) determines the spin Hall ratio in our Pt films. The variation of ξ_{DL}^E with t_{Pt} is consistent with an *effective* $\lambda_s^{\text{eff}} = 2.0 \pm 0.1$ nm, but this determination neglects the fact that spin relaxation in Pt is predicted to be dominated by the Elliott-Yafet (E-Y) mechanism [49,50], so that λ_s should scale linearly with $1/\rho_{\text{Pt}}$ and therefore the spin diffusion length should depend on t_{Pt} in our samples as well. We find that an analysis that assumes that $\lambda_s \rho_{\text{Pt}}$ is a constant in our bilayer samples fits the experimental results well, and from the fit we obtain $\lambda_s \rho_{\text{Pt}} = (0.77 \pm 0.08) \times 10^{-15} \Omega \cdot \text{m}^2$. As discussed below, taking into account that λ_s should scale $\propto 1/\rho_{\text{Pt}}$ would appear to resolve a prolonged controversy regarding the values of λ_s obtained from various SHE and ISHE experiments.

We studied multilayer samples consisting of *substrate*/Ta(1)/Pt(t_{Pt})/Co(1)/MgO(2)/Ta(1) (numbers in parentheses are thicknesses in nm) grown on oxidized Si substrates by sputter-deposition in a vacuum of $< 1.0 \times 10^{-7}$ Torr. The Ta(1) seeding layer resulted in a smoother multilayer [51,52] and enhanced perpendicular magnetic anisotropy (PMA) of the Co. The Pt thickness t_{Pt} , as averaged over the sample area, was varied in fine steps from 1.2 nm to 15 nm with a relative uncertainty of about 5%. This series of samples exhibit PMA with coercivity of ≈ 0.4 T without post-deposition annealing. The saturation magnetization is $M_s = (1.08 \pm 0.05) \times 10^6$ A/m with an apparent “magnetic dead layer” of $t_{\text{FM}}^{\text{dead}} = 0.26 \pm 0.04$ nm [29]. For the HR measurements, the multilayer stacks were patterned into

5 μm \times 60 μm Hall bars by photolithography and ion milling. All measurements were carried out at room temperature (RT).

The sheet conductances of the films were determined by 4-probe resistance measurements of a set of microbars of varying width, length and probe spacing, which minimized errors due to sample geometry and reduced the statistical measurement error to below 1%. Thus the main source of error comes from the uncertainty of film thicknesses. The resistivity of Pt layer ρ_{Pt} was determined by subtracting the sheet conductance of a separately fabricated Ta(1)/Co(1)/MgO(2)/Ta(1) stack from that of our samples containing the Pt layer. In Fig. 1(a) we show ρ_{Pt} for the samples as a function of t_{Pt} . The sharp increase of ρ_{Pt} with decreasing t_{Pt} is a well-known phenomenon due to strong diffusive scattering at a Pt surface [48,53–57].

The DL and FL SH torque efficiencies of these PMA samples were measured by the HR technique [20,29] with the same alternating voltage amplitude (4 V) applied to the Hall bars in all measurements, corresponding to an alternating electric field of constant magnitude $E = 67 \text{ kV/m}$. Fig. 1(b) shows the SH torque-induced longitudinal H_{L} (corresponding to DL torque) and transverse H_{T} (corresponding to FL torque) equivalent fields per unit applied electric field determined by the HR measurement as functions of t_{Pt} . As t_{Pt} increases, H_{L} quickly increases and then saturates for $t_{\text{Pt}} > 5 \text{ nm}$. H_{T} starts for t_{Pt} near zero from a value that is negative in our convention, opposite to the Oersted field generated by the charge current flow in the Pt, but quickly reaches a positive maximum and then decreases gradually. (We will discuss the details of our analysis of this H_{T} behavior elsewhere.) We determine the DL (FL) SH torque efficiencies *per unit applied current density* as

$$\xi_{\text{DL(FL)}}^j = \frac{2e}{\hbar} \mu_0 M_s (t_{\text{FM}} - t_{\text{FM}}^{\text{dead}}) \cdot H_{\text{L(T)}} / j_e \quad (3)$$

where $j_e = E / \rho_{\text{Pt}}$. Fig. 1(c) shows the DL and FL torque efficiencies per unit current density as functions of t_{Pt} . ξ_{DL}^j first increases with t_{Pt} and reaches a maximum ≈ 0.12 at $t_{\text{Pt}} = 2.8 - 3.9$ nm, but then, surprisingly, decreases gradually with t_{Pt} . The thickness dependence of ξ_{DL}^j that we observe is qualitatively similar to that observed in YIG/Pt bilayers [57] but quite different from other previous ferromagnetic resonance (FMR) measurements [38,40,44,45] and spin pumping/ISHE experiments [21–23] on metallic FM/Pt bilayers where the data typically are fit by a simple functional form [37]:

$$\xi_{\text{DL}}^j(t_{\text{NM}}) = \frac{2e}{\hbar} T_{\text{int}} j_s(t_{\text{NM}}) / j_e(t_{\text{NM}}) = \xi_{\text{DL,max}}^j (1 - \text{sech}(t_{\text{NM}} / \lambda_s)). \quad (4)$$

This is the behavior expected for an ideal ($T_{\text{int}} = 1$) interface with no SBF, or alternatively one where SML is the dominant cause for $T_{\text{int}} < 1$. However, we emphasize that Eq. (4) holds only under the assumption of constant ρ_{NM} and hence thickness-independent values for θ_{SH} and λ_s .

We note that an analysis that assumed constant θ_{SH} and λ_s could not explain the similar thickness-dependent behavior reported in Ref. [57]. In the intrinsic SHE regime, which has recently been reported to describe Pt [39,58], and also in the side-jump regime, it is the spin Hall conductivity σ_{SH} that is expected to be constant, independent of $\rho_{\text{NM}}(t_{\text{NM}})$ while the spin Hall ratio $\theta_{\text{SH}}(t_{\text{NM}}) = (2e / \hbar) \sigma_{\text{SH}} \rho_{\text{NM}}(t_{\text{NM}})$ should vary $\propto \rho_{\text{NM}}(t_{\text{NM}})$ and therefore ξ_{DL}^j also depends on the NM resistivity and hence, in this study, on its thickness due to strong interfacial scattering.

An alternative approach is to consider the spin torque efficiency *per unit applied electric field*, determined directly from the HR measurement as

$$\xi_{\text{DL}}^E = \frac{2e}{\hbar} \mu_0 M_s (t_{\text{FM}} - t_{\text{FM}}^{\text{dead}}) H_L / E. \quad (5)$$

The dependence of ξ_{DL}^E on Pt thickness is shown in Fig. 1(d) and is consistent with the functional form in Eq. (4) with a prefactor that does not depend on t_{Pt} , which indicates that the intrinsic SHE, or perhaps the side-jump mechanism, is indeed predominant in Pt. Then assuming that (i) the DL torque is entirely due to the SHE of the Pt, (ii) the interface is well ordered, and (iii) SBF is the dominant cause for $T_{\text{int}} < 1$, we can expect, approximately, [24,25]

$$\xi_{\text{DL}}^E(t_{\text{Pt}}) = \frac{2e}{\hbar} \sigma_{\text{SH}} (1 - \text{sech}(t_{\text{Pt}} / \lambda_s)) \left(1 + \frac{\tanh(t_{\text{Pt}} / \lambda_s)}{2\lambda_s \rho_{\text{Pt}} G_r} \right)^{-1}, \quad (6)$$

where G_r is the real part of the spin mixing conductance $G^{\uparrow\downarrow} = G_r + iG_i$ and we have assumed $G_r \gg G_i$, consistent with our result that $\xi_{\text{DL}} \ll \xi_{\text{FL}}$. As an exercise, if we fit the ξ_{DL}^E data shown in Fig. 1(d) to Eq. (6) using a fixed value $\rho_{\text{bulk}} = 15 \mu\Omega \cdot \text{cm}$, approximately the resistivity of the bulk Pt, and $G_r = 0.59 \times 10^{15} \Omega^{-1} \text{m}^{-2}$ as theoretically calculated for the Pt/Co interface [24], we obtain an ‘‘effective’’ spin diffusion length $\lambda_s^{\text{eff}} = 2.0 \pm 0.1 \text{ nm}$ and $\sigma_{\text{SH}} = (10.5 \pm 0.3) \times 10^5 [\hbar / 2e] \Omega^{-1} \cdot \text{m}^{-1}$ or $\theta_{\text{SH}} = \rho_{\text{bulk}} \sigma_{\text{SH}} = 0.16 \pm 0.01$, consistent with previous estimations [28,31]. The choice of G_r may change the estimation of σ_{SH} but has a very weak effect on λ_s^{eff} . The existence of a SML would introduce a constant factor < 1 to the right hand side of Eq. (6), thus would increase the estimated σ_{SH} but would not affect λ_s^{eff} . We note that this analysis neglects any possible negative SHE from the 1 nm Ta layer (see the discussion in the Supplementary Material [52]). We account for the maximum possible effect from the Ta within the experimental uncertainties indicated in Fig. 1(c,d).

Although λ_s^{eff} indicates the scale of the Pt thickness for which the spin current flowing to the FM/NM interface begins to saturate, it is only a phenomenological number since both thickness-independent ρ_{Pt} and λ_s are assumed in Eq. (6). In a more realistic approach, given the non-uniformity of resistivity across the layer, both θ_{SH} and λ_s will vary with location within the Pt film. In particular, since the E-Y mechanism [49,50] is expected to be the dominant spin scattering process in Pt [46,47], we should have $\lambda_s \propto 1/\rho_{\text{Pt}}$. Hence λ_s near the Pt interfaces (where ρ_{Pt} is large) should be smaller than in the bulk. This means that the effective $\lambda_s^{\text{eff}} = 2.0$ nm obtained above from the simplified Eq. (6) yields an underestimate of λ_s within the bulk of the Pt film.

We have found that it is possible to go beyond this type of approximate treatment and perform, using a simple rescaling, a quantitative calculation of the spin torque (including SBF) even for a heavy-metal layer with a nonuniform resistivity and spin diffusion length, as long as (a) the intrinsic mechanism of the SHE dominates spin current generation and (b) the E-Y mechanism dominates spin relaxation. Assuming that these two conditions hold, we can then use the experimental values of $\xi_{\text{DL}}^E(t_{\text{Pt}})$ and $\rho_{\text{Pt}}(t_{\text{Pt}})$ to obtain an estimate for the value of $\lambda_s \rho_{\text{Pt}}$.

We first assume, as an exercise, that the thickness-dependence of Pt resistivity is due only to surface scattering at the Pt/Co interface. We note that although a more careful investigation indicates that the Ta/Pt interface is the major source of surface scattering, as fully discussed in the Supplementary Material [52], the result we obtain below is the same when considering the scattering as occurring at either interface or even at both. From the series of $\rho_{\text{Pt}}(t_{\text{Pt}}^n)$ as a function of Pt thickness presented in Fig. 1(a), we divide each of the Pt films into a series of

adjacent “slices” of thickness l^i each of which has a different, but uniform, resistivity ρ_{Pt}^i and spin diffusion length λ_s^i . These divisions lead to the distribution of $\rho_{\text{Pt}}(z)$ as shown in Fig. 2(b), where the z -axis points normal to the layers with $z = 0$ starting at the Pt/Co interface. As fully discussed in the Supplementary Material [52], the spin transmission through the i -th slice is identical to that for an “effective” slice having a fixed spin diffusion length λ_s^0 , resistivity ρ_{Pt}^0 and a rescaled effective thickness $L^i = l^i \rho_{\text{Pt}}^i / \rho_{\text{Pt}}^0$ so that $\lambda_s^i \rho_{\text{Pt}}^i = \lambda_s^0 \rho_{\text{Pt}}^0$ which holds under the E-Y mechanism. Thus a Pt layer of thickness $t_{\text{Pt}}^n = \sum_{i=1}^n l^i$ (a combination of n slices) with non-uniform resistivity and spin diffusion length is equivalent to a uniform “effective” Pt film having a thickness $T_{\text{Pt}}^n = \sum_{i=1}^n L^i$, as schematically depicted in Fig. 2(a). Since the “effective” layers are chosen to have constant ρ_{Pt}^0 (we choose $15 \mu\Omega \cdot \text{cm}$) and λ_s^0 , we can fit the ξ_{DL}^E data versus the rescaled thickness T_{Pt} to Eq. (6), just substituting T_{Pt} instead of t_{Pt} . One important factor we need to consider is the location of the Pt/Co interface, which is not necessarily at $z = 0$. This is because a few atomic layers of Pt at each of the interfaces may be intermixed with the adjacent material, and/or in the case of the Pt/Co interface magnetized by the proximity effect [59]. This can result in a small offset t_{off} because the thickness of the first slice is smaller than its nominal value. This effect seems to be apparent in Fig. 1(d) where the fitted line (which goes through the origin) does not fit the data particularly well in the thin Pt region. We address this issue in our analysis by replacing T_{Pt} in the right hand side of Eq. (6) by $T_{\text{Pt}} - T_{\text{off}}$ where T_{off} is the location of the FM/NM interface and is estimated from the fitting.

The fitted result of the “effective” Pt layers with three free parameters σ_{SH} , λ_s^0 and T_{off} is shown in Fig. 2(c). We obtain $\lambda_s^0 = 5.1 \pm 0.5 \text{ nm}$ for $\rho_{\text{Pt}}^0 = 15 \mu\Omega\text{cm}$, or more generally we

have $\lambda_s \rho_{\text{Pt}} = (0.77 \pm 0.08) \times 10^{-15} \text{ } \Omega \cdot \text{m}^2$; $T_{\text{off}} = 4.9 \pm 0.3 \text{ nm}$ for the “effective” Pt thickness offset which corresponds to $t_{\text{off}} = 0.8 \pm 0.1 \text{ nm}$ in the original, un-scaled thickness; and $\sigma_{\text{SH}} = (5.9 \pm 0.2) \times 10^5 [\hbar / 2e] \Omega^{-1} \text{m}^{-1}$ independent of ρ_{Pt} . If we use a somewhat higher $G_r = 1.07 \times 10^{15} \text{ } \Omega^{-1} \text{m}^{-2}$ as calculated including spin orbit effects for the Py/Pt interface [47] then $\sigma_{\text{SH}} = (4.5 \pm 0.1) \times 10^5 [\hbar / 2e] \Omega^{-1} \cdot \text{m}^{-1}$, again a lower bound. We reiterate that the existence of SML would increase the estimated σ_{SH} but negligibly affect our determination of λ_s^0 . As a final check of this analysis we note the requirement of the E-Y mechanism that the spin relaxation time τ_s be longer than the momentum scattering time τ_m . It has been reported that the mean free path l_{mfp} in Pt can be estimated from $l_{\text{mfp}} [\text{m}] \approx 8 \times 10^{-16} / \rho_{\text{Pt}} [\Omega \cdot \text{m}]$ [60]. Thus we have

$$\tau_{sf} / \tau_m = 3(\lambda_s / l_{\text{mfp}})^2 \approx 3 \left[\lambda_s \rho_{\text{Pt}} / (8 \times 10^{-16}) \right]^2 = 2.8, \quad (7)$$

which is consistent with the E-Y spin scattering mechanism being dominant in Pt.

We now discuss our results in relation with previous results in the literature. First, as noted above, previous ST-FMR and ISHE studies on in-plane magnetized (IPM) Pt/Py bilayers [38,40,44] did not yield a peak in the apparent damping-like spin torque efficiency as a function of t_{Pt} such as reported here. These previous analyses also reported a short $\lambda_s \approx 1.4 \text{ nm}$ as determined by RT ST-FMR, or alternatively by ISHE, on Py/Pt [38,40,44] and $\lambda_s \approx 2.1 \text{ nm}$ for $\text{Co}_{75}\text{Fe}_{25}/\text{Pt}$ [45], in the same range as $\lambda_s^{\text{eff}} = 2.0 \text{ nm}$. These differences with our results can be explained by a weaker thickness dependence of the resistivity for multilayers made from different materials and the neglect of any field-like torque in the analysis. See the Supplementary Material [52] for further discussion on these points.

An alternative approach to estimate λ_s is to measure the t_{Pt} dependence of Gilbert magnetic damping in bilayer samples, and such a study has recently reported $\lambda_s = 0.5 \pm 0.3$ nm [42]. Fast saturation of the damping at very thin Pt thicknesses has also been observed previously [22,37,38]. However, Liu *et al.* [47] have recently pointed out that this very rapid attenuation is likely due to strong SML at the FM/Pt interface, and used a first principles calculation and data [61] from this measurement method to obtain $\lambda_s \approx 5.5$ nm, or more generally $\lambda_s \rho_{\text{Pt}} = (0.61 \pm 0.02) \times 10^{-15} \Omega \cdot \text{m}^2$. On the other hand, a longer $\lambda_s \approx 8.0$ nm has been reported [21,22] from ISHE experiments on Py/Pt at RT. However, these latter works did not consider SML or spin backflow at the FM-NM interface which would reduce their estimated values, as pointed out by Jiao *et al.* [43]. Rojas-Sanchez *et al.* [23] performed similar measurement on Co/Pt and, after taking SML into account, reported $\lambda_s = 3.4 \pm 0.4$ nm and $\lambda_s \rho_{\text{Pt}} = (0.59 \pm 0.06) \times 10^{-15} \Omega \cdot \text{m}^2$. These experiments did not consider the non-uniformity of the local resistivity $\rho_{\text{Pt}}(t_{\text{Pt}})$ and its effect on $\lambda_s(t_{\text{Pt}})$, and thus underestimated the value of $\lambda_s \rho_{\text{Pt}}$. A very high value $\lambda_s = 11 \pm 2$ nm has been determined from a low temperature, 3-10 K, study of spin pumping in lateral spin valves [39,41] for samples having $\rho_{\text{Pt}} = 12 \mu\Omega \cdot \text{cm}$, or $\lambda_s \rho_{\text{Pt}} = 1.32 \times 10^{-15} \Omega \cdot \text{m}^2$. However, Isasa *et al.* used a similar lateral spin value technique and reported $\lambda_s \rho_{\text{Pt}} = (0.85 \pm 0.08) \times 10^{-15} \Omega \cdot \text{m}^2$ at 10 K and $(0.79 \pm 0.87) \times 10^{-15} \Omega \cdot \text{m}^2$ at RT [58], while measurements using current-perpendicular to the plane studies of Py-based exchange biased spin valves [26] at 4.2 K have reported $\lambda_s \rho_{\text{Pt}} = (0.59 \pm 0.25) \times 10^{-15} \Omega \cdot \text{m}^2$ [37] and $(0.72 \pm 0.13) \times 10^{-15} \Omega \cdot \text{m}^2$ [46]. All of these latter results, which were all obtained with Pt layers ~ 15 nm thick and therefore not susceptible to the non-uniform distribution of local resistivity as

in thinner Pt layers, are in reasonable agreement with our result

$$\lambda_s \rho_{\text{Pt}} = (0.77 \pm 0.08) \times 10^{-15} \Omega \cdot \text{m}^2.$$

In summary, we have observed a strong dependence on t_{Pt} for the damping-like SH torque efficiency per unit applied current density for perpendicularly-magnetized Pt/Co bilayer structures, with a peak value $\xi_{\text{DL}}^j = 0.12$ at $t_{\text{Pt}} = 2.8 - 3.9$ nm, while the spin torque efficiency per unit applied electric field exhibits a monotonic increase with increasing Pt thickness and saturates for $t_{\text{Pt}} > 5$ nm. We interpret this behavior as an indication that the intrinsic mechanism for the SHE being dominant in Pt, perhaps in combination with side-jump scattering, so that the SH conductivity is independent of mean free path while the SH torque efficiency per unit current density is enhanced by an increased $\rho_{\text{Pt}}(t_{\text{Pt}})$ associated with interfacial scattering. By assuming the E-Y mechanism for spin scattering, which implies that $\lambda_s \propto 1/\rho_{\text{Pt}}$ so that λ_s is also non-uniform, we obtain $\lambda_s \rho_{\text{Pt}} = (0.77 \pm 0.08) \times 10^{-15} \Omega \cdot \text{m}^2$. With this result we can apply SBF analysis to our direct measurements of ξ_{DL}^E for this PMA system using $G_r = 0.59 \times 10^{15} \Omega^{-1} \text{m}^{-2}$ [24], and obtain $\sigma_{\text{SH}}^{\text{Pt}} = (5.9 \pm 0.2) \times 10^5 [\hbar/2e] \Omega^{-1} \cdot \text{m}^{-1}$, with this being a lower bound as it is made with the assumption that there is no significant SML at our Pt/Co interfaces.

This work seems to resolve the controversy regarding the differences in the value of λ_s for Pt as obtained from various spin Hall and other experiments, and demonstrates that the spin Hall efficiency of Pt can be enhanced by increasing its resistivity, as expected when the intrinsic SHE is dominant.

Acknowledgments

We thank Y. Ou, C.-F. Pai and S. Emori for fruitful discussions, G. E. Rowlands for technical support and F. Guo for commenting on the manuscript. This work was supported in part by the Samsung Electronics Corporation, by the NSF/MRSEC program (DMR-1120296) through, the Cornell Center for Materials Research, and by ONR. We also acknowledge support from the NSF (Grant No. ECCS- 1542081) through use of the Cornell Nanofabrication Facility/National Nanofabrication Infrastructure Network.

REFERENCES

- [1] M. I. Dyakonov and V. I. Perel, *Phys. Letters* **35A**, (1971).
- [2] J. Hirsch, *Phys. Rev. Lett.* **83**, 1834 (1999).
- [3] S. Zhang, *Phys. Rev. Lett.* **85**, 393 (2000).
- [4] C.-F. Pai, L. Liu, Y. Li, H. W. Tseng, D. C. Ralph, and R. A. Buhrman, *Appl. Phys. Lett.* **101**, 122404 (2012).
- [5] L. Liu, C.-F. Pai, D. C. Ralph, and R. A. Buhrman, *Phys. Rev. Lett.* **109**, 186602 (2012).
- [6] V. E. Demidov, S. Urazhdin, H. Ulrichs, V. Tiberkevich, A. Slavin, D. Baither, G. Schmitz, and S. O. Demokritov, *Nat. Mater.* **11**, 1028 (2012).
- [7] V. E. Demidov, H. Ulrichs, S. V Gurevich, S. O. Demokritov, V. S. Tiberkevich, a N. Slavin, a Zholud, and S. Urazhdin, *Nat. Commun.* **5**, 3179 (2014).
- [8] T. Jungwirth, J. Wunderlich, and K. Olejník, *Nat. Mater.* **11**, 382 (2012).
- [9] P. P. J. Haazen, E. Murè, J. H. Franken, R. Lavrijsen, H. J. M. Swagten, and B. Koopmans, *Nat. Mater.* **12**, 299 (2013).
- [10] N. Okamoto, H. Kurebayashi, T. Trypiniotis, I. Farrer, D. A. Ritchie, E. Saitoh, J. Sinova, J. Mašek, T. Jungwirth, and C. H. W. Barnes, *Nat. Mater.* **13**, 932 (2014).
- [11] D. Bhowmik, L. You, and S. Salahuddin, *Nat. Nanotechnol.* **9**, 59 (2013).
- [12] D. M. Bromberg, D. H. Morris, L. Pileggi, and J.-G. Zhu, *IEEE Trans. Magn.* **48**, 3215 (2012).
- [13] S. Urazhdin, V. E. Demidov, H. Ulrichs, T. Kendziorczyk, T. Kuhn, J. Leuthold, G. Wilde, and S. O. Demokritov, *Nat. Nanotechnol.* **9**, 509 (2014).
- [14] G. Vignale, *J. Supercond. Nov. Magn.* **23**, 3 (2010).
- [15] A. Hoffmann, *IEEE Trans. Magn.* **49**, 5172 (2013).
- [16] R. Karplus and J. M. Luttinger, *Phys. Rev.* **95**, 1154 (1954).
- [17] L. Berger, *Phys. Rev. B* **2**, 4559 (1970).
- [18] J. Smit, *Physica* **24**, 39 (1958).
- [19] L. Liu, C.-F. Pai, Y. Li, H. W. Tseng, D. C. Ralph, and R. A. Buhrman, *Science* **336**, 555 (2012).
- [20] J. Kim, J. Sinha, M. Hayashi, M. Yamanouchi, S. Fukami, T. Suzuki, S. Mitani, and H. Ohno, *Nat. Mater.* **12**, 240 (2013).
- [21] H. Nakayama, K. Ando, K. Harii, T. Yoshino, R. Takahashi, Y. Kajiwara, K. Uchida, Y. Fujikawa, and E. Saitoh, *Phys. Rev. B* **85**, 144408 (2012).
- [22] Z. Feng, J. Hu, L. Sun, B. You, D. Wu, J. Du, W. Zhang, A. Hu, Y. Yang, D. M. Tang, B. S. Zhang, and H. F. Ding, *Phys. Rev. B* **85**, 214423 (2012).

- [23] J.-C. Rojas-Sánchez, N. Reyren, P. Laczkowski, W. Savero, J.-P. Attané, C. Deranlot, M. Jamet, J.-M. George, L. Vila, and H. Jaffrès, *Phys. Rev. Lett.* **112**, 106602 (2014).
- [24] P. M. Haney, H.-W. Lee, K.-J. Lee, A. Manchon, and M. D. Stiles, *Phys. Rev. B* **87**, 174411 (2013).
- [25] Y.-T. Chen, S. Takahashi, H. Nakayama, M. Althammer, S. Goennenwein, E. Saitoh, and G. Bauer, *Phys. Rev. B* **87**, 144411 (2013).
- [26] W. Park, D. Baxter, S. Steenwyk, I. Moraru, W. Pratt, and J. Bass, *Phys. Rev. B* **62**, 1178 (2000).
- [27] L. Liu, T. Moriyama, D. C. Ralph, and R. A. Buhrman, *Phys. Rev. Lett.* **106**, 036601 (2011).
- [28] M.-H. Nguyen, C.-F. Pai, K. X. Nguyen, D. A. Muller, D. C. Ralph, and R. A. Buhrman, *Appl. Phys. Lett.* **106**, 222402 (2015).
- [29] C.-F. Pai, Y. Ou, L. H. Vilela-leão, D. C. Ralph, and R. A. Buhrman, *Phys. Rev. B* **92**, 064426 (2015).
- [30] L. Liu, C.-T. Chen, and J. Z. Sun, *Nat. Phys.* **10**, 561 (2014).
- [31] W. Zhang, W. Han, X. Jiang, S.-H. Yang, and S. S. P. Parkin, *Nat. Phys.* **11**, 496 (2015).
- [32] X. Fan, J. Wu, Y. Chen, M. J. Jerry, H. Zhang, and J. Q. Xiao, *Nat. Commun.* **4**, 1799 (2013).
- [33] X. Fan, H. Celik, J. Wu, C. Ni, K.-J. Lee, V. O. Lorenz, and J. Q. Xiao, *Nat. Commun.* **5**, 3042 (2014).
- [34] T. Nan, S. Emori, C. T. Boone, X. Wang, T. M. Oxholm, J. G. Jones, B. M. Howe, G. J. Brown, and N. X. Sun, *Phys. Rev. B* **91**, 214416 (2015).
- [35] T. D. Skinner, M. Wang, A. T. Hindmarch, A. W. Rushforth, A. C. Irvine, D. Heiss, H. Kurebayashi, and A. J. Ferguson, *Appl. Phys. Lett.* **104**, 062401 (2014).
- [36] K. Garello, I. M. Miron, C. O. Avci, F. Freimuth, Y. Mokrousov, S. Blügel, S. Auffret, O. Boulle, G. Gaudin, and P. Gambardella, *Nat. Nanotechnol.* **8**, 587 (2013).
- [37] H. Kurt, R. Loloee, K. Eid, W. P. Pratt, and J. Bass, *Appl. Phys. Lett.* **81**, 4787 (2002).
- [38] L. Liu, R. A. Buhrman, and D. C. Ralph, *arXiv:1111.3702* (2011).
- [39] M. Morota, Y. Niimi, K. Ohnishi, D. H. Wei, T. Tanaka, H. Kontani, T. Kimura, and Y. Otani, *Phys. Rev. B* **83**, 174405 (2011).
- [40] K. Kondou, H. Sukegawa, S. Mitani, K. Tsukagoshi, and S. Kasai, *Appl. Phys. Express* **5**, 073002 (2012).
- [41] Y. Niimi, D. Wei, H. Idzuchi, T. Wakamura, T. Kato, and Y. Otani, *Phys. Rev. Lett.* **110**, 016805 (2013).
- [42] C. T. Boone, H. T. Nembach, J. M. Shaw, and T. J. Silva, *J. Appl. Phys.* **113**, 153906 (2013).

- [43] H. Jiao and G. E. W. Bauer, *Phys. Rev. Lett.* **110**, 217602 (2013).
- [44] W. Zhang, V. Vlaminck, J. E. Pearson, R. Divan, S. D. Bader, and A. Hoffmann, *Appl. Phys. Lett.* **103**, 242414 (2013).
- [45] A. Ganguly, K. Kondou, H. Sukegawa, S. Mitani, S. Kasai, Y. Niimi, Y. Otani, and A. Barman, *Appl. Phys. Lett.* **104**, 072405 (2014).
- [46] H. Y. T. Nguyen, W. P. Pratt, and J. Bass, *J. Magn. Magn. Mater.* **361**, 30 (2014).
- [47] Y. Liu, Z. Yuan, R. J. H. Wesselink, A. A. Starikov, and P. J. Kelly, *Phys. Rev. Lett.* **113**, 207202 (2014).
- [48] C. T. Boone, J. M. Shaw, H. T. Nembach, and T. J. Silva, *J. Appl. Phys.* **117**, 223910 (2015).
- [49] R. J. Elliott, *Phys. Rev.* **96**, 266 (1954).
- [50] Y. Yafet, *Solid State Phys.* **14**, 1 (1963).
- [51] J. M. Shaw, H. T. Nembach, T. J. Silva, S. E. Russek, R. Geiss, C. Jones, N. Clark, T. Leo, and D. J. Smith, *Phys. Rev. B* **80**, 184419 (2009).
- [52] See Supplementary Material [URL], which includes Ref. [62], for further discussion on the rescaling method, the previously reported ST-FMR studies and the effect of the Ta seeding layer.
- [53] A. F. Mayadas and M. Shatzkes, *Phys. Rev. B* **1**, 1382 (1970).
- [54] F. Warkusz, *Electrocompon. Sci. Technol.* **5**, 99 (1978).
- [55] H. D. Liu, Y. P. Zhao, G. Ramanath, S. P. Murarka, and G. C. Wang, *Thin Solid Films* **384**, 151 (2001).
- [56] W. E. Bailey, S. X. Wang, and E. Y. Tsybal, *Phys. Rev. B* **61**, 1330 (2000).
- [57] V. Castel, N. Vlietstra, J. Ben Youssef, and B. J. Van Wees, *Appl. Phys. Lett.* **101**, 132414 (2012).
- [58] M. Isasa, E. Villamor, L. E. Hueso, M. Gradhand, and F. Casanova, *Phys. Rev. B* **91**, 024402 (2014).
- [59] S. Y. Huang, X. Fan, D. Qu, Y. P. Chen, W. G. Wang, J. Wu, T. Y. Chen, J. Q. Xiao, and C. L. Chien, *Phys. Rev. Lett.* **109**, 107204 (2012).
- [60] J. Bass and W. P. Pratt, *J. Phys. Condens. Matter* **19**, 183201 (2007).
- [61] S. Mizukami, Y. Ando, and T. Miyazaki, *Phys. Rev. B* **66**, 104413 (2002).
- [62] P. C. Van Son, H. Van Kempen, and P. Wyder, *Phys. Rev. Lett.* **58**, 2271 (1987).

FIGURES

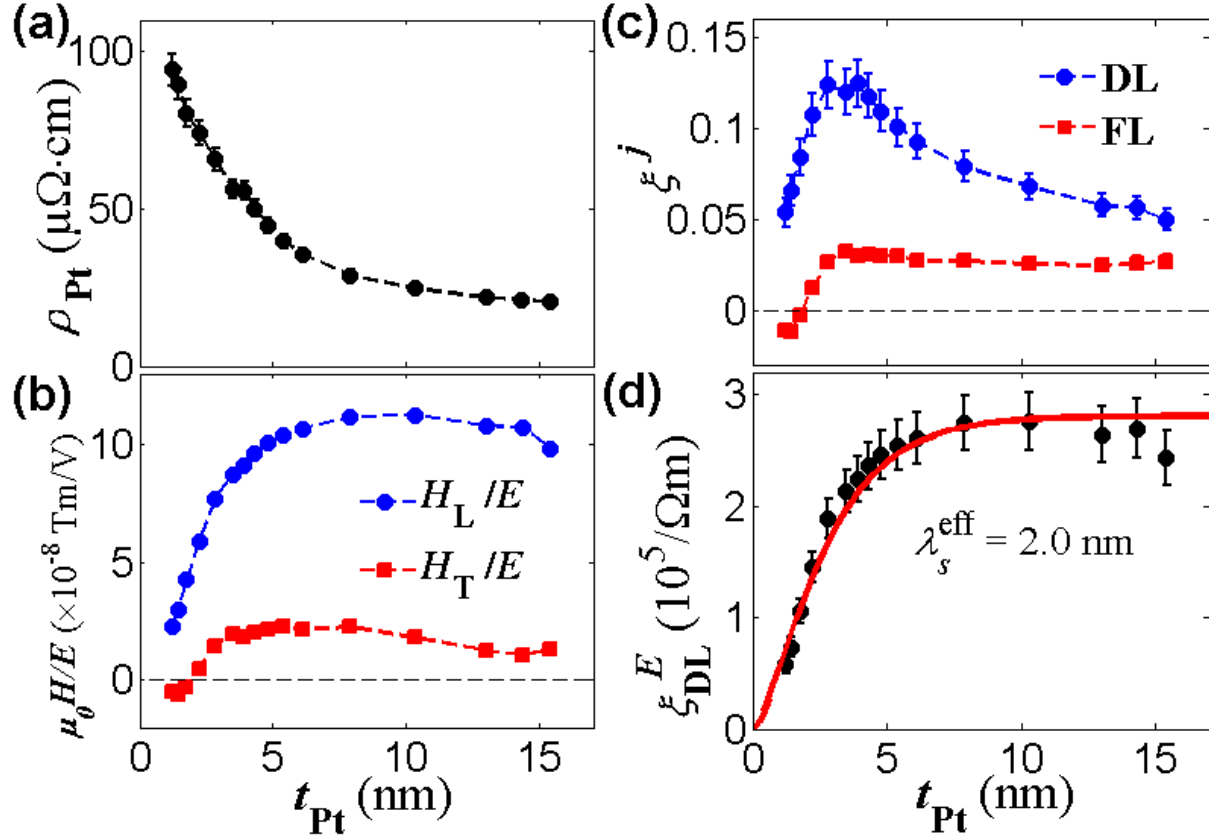


Figure 1: (Color online) **(a)** Resistivity of Pt in Ta(1)/Pt/Co(1), **(b)** SH torque-induced longitudinal (circles) and transverse (squares) equivalent fields per unit applied electric field, **(c)** damping-like (circles) and field-like (squares) SH torque efficiency per unit applied current density, and **(d)** damping-like SH torque efficiency per unit applied electric field as functions of Pt thickness. The solid line in (d) shows the fitted result to equation (4) from which the *effective* spin diffusion length is estimated to be $\lambda_s^{\text{eff}} = 2.0 \pm 0.1$ nm. The broken lines in other plots connect the data points.

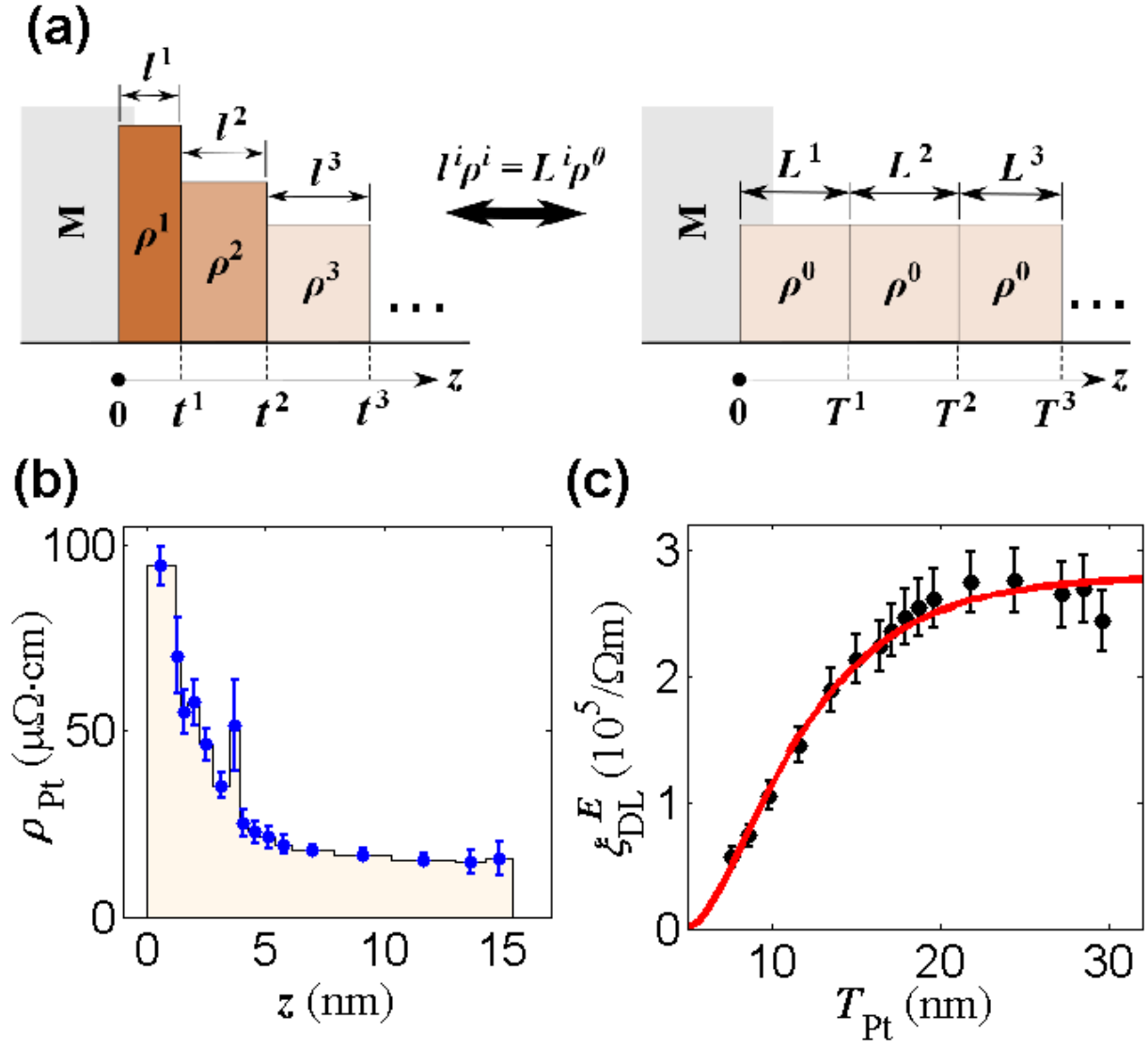


Figure 2: (Color online) Estimation of spin diffusion length within the E-Y mechanism. **(a)** Schematic illustration of the “slicing” and “rescaling” process in which a non-uniform layer t_{Pt}^n is scaled into a uniform one T_{Pt}^n . See full description in the main text. **(b)** The distribution of Pt local resistivity with location z , extracted from the experimental Ta/Pt/Co data in Fig. 1(a). The points represent the local resistivity of each “slice”. **(c)** Damping-like spin torque efficiency per unit applied electric field versus “effective” thickness T_{Pt} . The solid line shows the fitted result from which the spin diffusion length of Pt at $\rho_{\text{Pt}}^0 = 15 \mu\Omega \cdot \text{cm}$ is estimated to be $\lambda_s^0 = 5.1 \pm 0.5 \text{ nm}$.